



Sonocatalytic Fe₃O₄ cluster microspheres/g-C₃N₄ composite for efficient removal of organic dyes

Nguyen Xuan Sang¹, Nguyen Thi Hong Phuong²

¹Environmental Institute, Viet Nam Maritime University, Hai Phong, Viet Nam

²Hanoi University of Science and Technology, Hanoi, Viet Nam

*Email: sangnx.vmt@vimaru.edu.vn

ARTICLE INFO

Received: 04/7/2023

Accepted: 15/12/2023

Published: 30/3/2024

Keywords:

Cluster microsphere Fe₃O₄; sonocatalytic; composite; dye degradation

ABSTRACT

In this study, Fe₃O₄/g-C₃N₄ composite was fabricated via facile hydrothermal techniques. The Fe₃O₄/g-C₃N₄ product was used as catalysts for degradation of methylene blue (MB), rhodamine B (RhB) and methyl orange (MO) degradation with ultrasonic-assisted and H₂O₂. To characterize the structure and morphology of the as-prepared product the X-ray diffraction (XRD) and scanning electron microscopy (SEM) were examined. The integration of H₂O₂ and catalyst dosage enhanced the sonocatalytic degradation of dyes. The catalysts after reaction can easily be separated and reused with external magnetic fields. The experimental results show that catalytic activity of as-synthesized Fe₃O₄/g-C₃N₄ decreased insignificantly in the dye degradation after four recycles.

1. Introduction

Recently, organic chemical dye is used widely in many industrial fields such as pharmaceuticals, textile printing and paper. Release of the toxic industry in wastewater may cause pollution the biological systems and water resources. However, conventional treatment methods could not effectively degrade and mineralize organic dyes [1, 2]. With high oxidation activity through generation of hydroxyl radicals, advanced oxidation processes (AOPs) have been used widely for dye organic degradation. Nowadays, sonication often is used as an assistant for improving the catalytic process because of generating physical and chemical effects, such as promoting mass transfer and active radical formation. Sound waves at high frequency (above 20 kHz) called ultrasound have been paid great attention due to their benefit catalysis in multiple ways. Ultrasonic has been employed in material synthesis techniques for adjusting physico-chemical properties

and enhancing reaction efficiency [3, 4]. The ultrasound assistant in field-improved catalytic technology can be attributed to a nucleation microbubbles, resulting in the formation of radicals species such as OOH•, OH•, HO₂• [5, 6]. Due to the simple operation and low cost, the combination of a Fenton-like process and ultrasound irradiation is considered as a promising AOP for water and wastewater treatment [7]. However, application by only ultrasonic, efficiency of the organic contaminant removal process is not high, leading to wasting energy and time [8]. So, coupling the catalytic with ultrasonic is a new approach to solve this issue. Various catalysts such as CuS, TiO₂, ZnTiO₃, Er doped ZnO have exposed high sono-catalytic activities [9, 10]. However, developing new magnetic composite sonocatalysts with high catalytic activity, easily separated and reused is still a challenge [11].

Graphitic carbon (g-C₃N₄) has attracted great attention for many applications because of their unique physicochemical property and stable allotrope. With the structure of a two-dimensional framework, g-C₃N₄ exhibits basic surface sites, electron-rich sites and highly stable hydrothermal and chemical stability [12]. The properties play an important role in catalytic application. Fe₃O₄ with cubic spinel structure have emerged as a promising material for various fields due to their abundant, interesting magnetic property, high catalytic activity, and friendly environment [13]. It was reported that synthesis of Fe₃O₄ nanoparticles with desired structure, composition and controllable shape can accelerate the electron transfer and generate the radical species, improving catalytic activity.

Loading magnetic materials on carbon nitrides have been developed as a promising approach to improve the catalytic activity, reuse and recovery ability [14, 15]. In the present study, application the magnetic Fe₃O₄ cluster spheres/g-C₃N₄ as a new sono-catalyst for an efficient H₂O₂-assisted sono-degradation of rhodamine B (RhB), methyl blue (MB) and methyl orange (MO) in aqueous solutions were reported. This sonocatalyst composite was prepared through a simple hydrothermal method. In addition, a proposed mechanism for dyes ultrasonic-assisted degradation with Fe₃O₄ cluster spheres catalyst and presence of H₂O₂ was discussed.

2. Experimental

Synthesis of composites

Melamine was used as a precursor for synthesis of pure g-C₃N₄. Typically, melamine was put in a muffle furnace powder at 550 °C for 4h [12,15]. Then, obtained products were collected and washed with deionized water several times for further use. The Fe₃O₄/g-C₃N₄ catalyst was synthesized using a simple hydrothermal procedure. In a typical process, 0.5g of g-C₃N₄ and 2.04 g of Fe(NO₃)₃.9H₂O were mixed in 60ml of deionized water. The solution was stirred for 30 minutes by a magnetic stirring at room temperature. Before putting into a Teflon-lined autoclave, 10mL of sodium alginate solution (10g/L) and 10ml KOH (2M) was introduced into the solution. After 30 min ultrasonic treatment (at frequency of 25kHz with a power dissipation of 80 W), the mixture was transferred into a Teflon liner of 100mL capability and hydrothermal at 180°C for 12h and cooled to room temperature naturally. The precipitate was separated

by filtration, then washed with ethanol distilled water several times. The resulting powder was dried in an oven at 80°C for 10h to obtain dry powdered Fe₃O₄/g-C₃N₄ material.

Characterization

Several analyses were used to discover the identification and characterization of the as-prepared product. X-ray diffraction (XRD) was carried out to examine the phase composition and crystalline structure. Transmission electron microscopy (FESEM-JEM 2100F) was used to check the morphology, composite structure. The absorption spectra of dye during the degradation process was determined using a UV-Vis spectrophotometer (shimadzu UV 1750, Japan).

The sonocatalytic degradation

The sonocatalytic degradation processes were investigated by measuring the decoloration of dye solution. RhB, MB, and MO were employed as typical pollutants to examine the sono degradation capacity of the as-synthesized composites. The dyes solution of 10 mg/L was prepared as a standard stock solution. Then, 0.1g of Fe₃O₄/g-C₃N₄ composite was introduced into 50mL of the dye aqueous solution. The mixture was stirred for 30 minutes in the dark to obtain the equilibrium adsorption and desorption. Then, 0.1ml of the H₂O₂ aqueous solution (30%) was added to the system. To investigate the catalytic activity with ultrasonic-assisted treatment, the mixed solution was then placed inside a bath (EYG-3003). The ultrasonic frequency was fixed at 40kHz with a power dissipation of 80 W and room temperature. After every 30 minutes about 5ml of the solution was taken out from the system. The collected suspension was centrifuged to remove the catalyst powder. The UV-vis spectrum of solution was measured using the UV-Vis spectrophotometer.

3. Results and discussion

XRD analysis

X-ray diffraction patterns of g-C₃N₄, Fe₃O₄, and Fe₃O₄ clusters/g-C₃N₄ 20% wt are depicted in Fig. 1. As shown in Fig. 1, all the diffraction peaks and positions of pure Fe₃O₄ and Fe₃O₄ clusters/g-C₃N₄ composite can be indexed to the cubic Fe₃O₄ (JCPDS 86-1354). The strong and sharp diffraction peaks can clearly be

observed on the XRD spectra of Fe_3O_4 cluster microspheres indicating their high crystallinity structure [16]. The two main peaks of $\text{g-C}_3\text{N}_4$ located at 13.28 and 27.33 indexing to (100) and (002) diffraction planes (JCPDS 87-1526). Compared to pure $\text{g-C}_3\text{N}_4$, most peaks observing for $\text{Fe}_3\text{O}_4/\text{g-C}_3\text{N}_4$ can be indexed to the structure of Fe_3O_4 . In the XRD pattern of $\text{Fe}_3\text{O}_4/\text{g-C}_3\text{N}_4$ composite sample, the characteristic peaks of $\text{g-C}_3\text{N}_4$ could not be exposed. This can be explained that the presence of Fe_3O_4 affected to the appearance of these peaks, resulting in the main peak of $\text{g-C}_3\text{N}_4$ becoming weaker. This can be attributed to the interference of Fe_3O_4 leading to the diffraction peaks of $\text{g-C}_3\text{N}_4$ are largely attenuated. The results are well agreed with the previous reported in literature [17,18]. The results indicates the composites were formed between $\text{g-C}_3\text{N}_4$ and Fe_3O_4 cluster spheres.

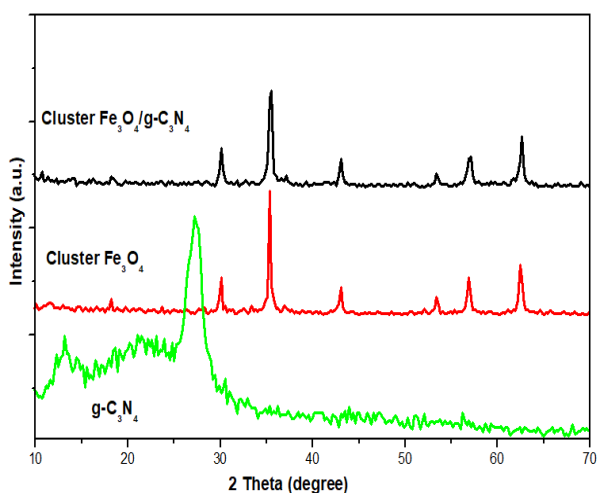


Fig. 1: XRD pattern of $\text{g-C}_3\text{N}_4$, cluster Fe_3O_4 , and $\text{Fe}_3\text{O}_4/\text{g-C}_3\text{N}_4$

SEM analysis

To investigate the surface properties of pure cluster sphere Fe_3O_4 and Fe_3O_4 cluster spheres/ $\text{g-C}_3\text{N}_4$ composite catalyst SEM analysis was conducted. The SEM results can be observed in Fig. 2. As depicted in Fig. 2a, the as-prepared pure Fe_3O_4 product comprises micro-spherical particles with well-dispersed. The particles exhibit a high uniform in size and shape with the average particle size of around 300-500nm. In addition, the SEM image of spherical particles reveals that these Fe_3O_4 particles have hierarchical architecture structure and were mainly composed of many single crystallites of approximately 30-40nm in size by the ordered assembly. The average crystallite size observed from the SEM image agrees well with the result calculated by Debye-Scherrer equation from the XRD pattern.

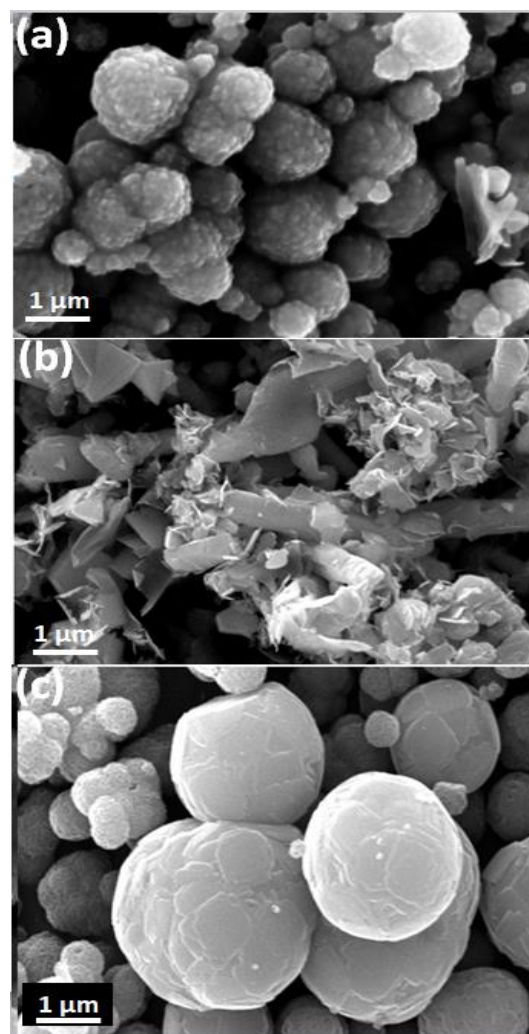


Fig. 2: SEM image of Fe_3O_4 cluster spheres (a); $\text{g-C}_3\text{N}_4$ (b), and $\text{Fe}_3\text{O}_4/\text{g-C}_3\text{N}_4$ composites (c)

Based on the above SEM image, it can clearly be seen that the pure Fe_3O_4 are colloidal nanocrystal clusters. As depicted in Fig. 2b, the SEM of the pure $\text{g-C}_3\text{N}_4$ showing the characteristic lamellar layered and planar structure for the graphitic pure of carbon nitride. From Fig. 2c, it is seen that when Fe_3O_4 clusters were modified with the $\text{g-C}_3\text{N}_4$, the morphology of the obtained product changed and became less porosity. It can be attributed to covering the surface of Fe_3O_4 by $\text{g-C}_3\text{N}_4$ particles. The accommodation of $\text{g-C}_3\text{N}_4$ on the surface of Fe_3O_4 forms a tight heterostructure. In this case, close interaction between two phases of $\text{g-C}_3\text{N}_4$ and Fe_3O_4 are leading to formation of an intimate interface [19-21]. It is said that the use of ultrasonic assisted methods in catalyst synthesis may improve the generation, growth and collapse of microbubbles. These cavitations play an important role in preparing heterostructure materials, leading to encourage the formation of the stable hybrid structure between $\text{g-C}_3\text{N}_4$ and Fe_3O_4 composite [22].

Sonocatalytic degradation of dye

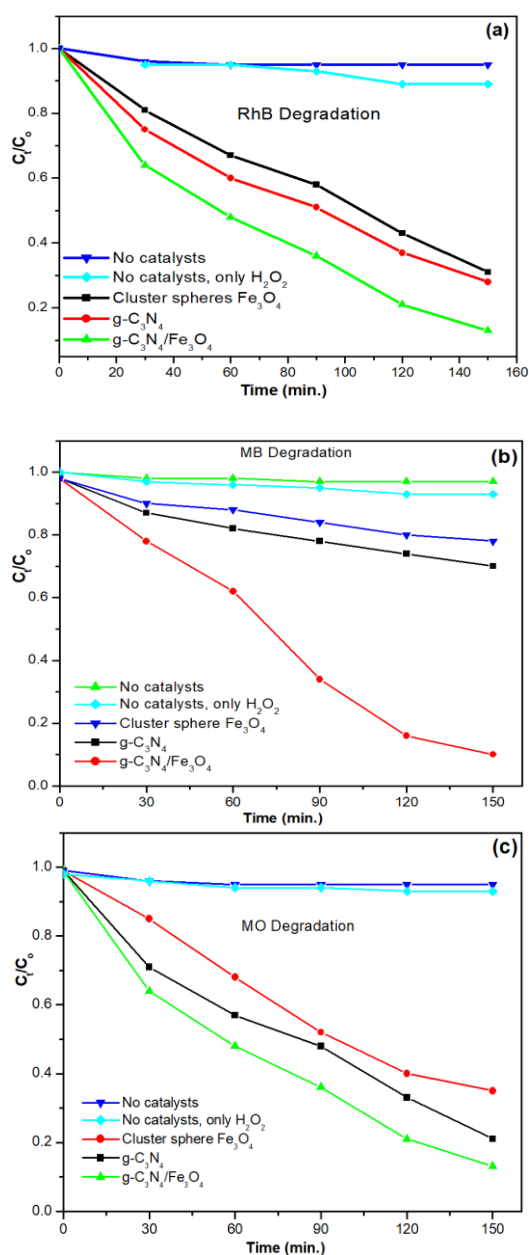


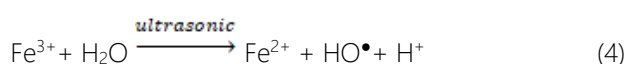
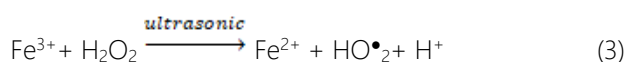
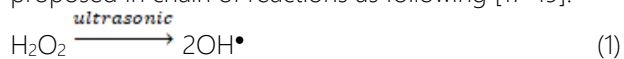
Fig. 3: The dye sono-degradation with different conditions for (a) RhB degradation; (b) MB degradation; (c) MO degradation

The sonocatalytic activity of the Fe₃O₄/g-C₃N₄ catalysts were evaluated through the degradation of RhB, MB, and MO in the presence of H₂O₂ with ultrasonic irradiation. The results of sonocatalytic activities of the as-synthesized catalyst at different conditions are depicted in Fig. 3. No dye degradation can be observed without catalytic. The sonocatalytic activity of the cluster Fe₃O₄/g-C₃N₄ composite is further examined by comparison with that of pure two-component. Compared with only sonolysis or only H₂O₂, the degradation of dyes were enhanced using

catalysts and ultrasonic-assisted processes. The dye removal rate of only sonolysis/H₂O₂, and sonocatalysis using g-C₃N₄/H₂O₂, Fe₃O₄/H₂O₂, Fe₃O₄/g-C₃N₄/H₂O₂ systems was 3%, 7%, 64%, 22 % and 96.5% within reaction time of 150 min for RhB, respectively. Cluster Fe₃O₄/g-C₃N₄ composite is much more efficient than pure cluster sphere Fe₃O₄ and pure g-C₃N₄ (Fig. 3a). The sonocatalytic processes for MB and MO degradation show the same results as depicted in Fig. 3b and Fig. 3c.

To identified the catalytic activity of cluster sphere Fe₃O₄/g-C₃N₄ composite for dye degradation, the major peaks for RB ($\lambda=546$ nm), MB ($\lambda=665$ nm) and MO ($\lambda=463$ nm) were measured. The results show in Fig. 4. The intensity of the characteristic peak of Rh, MB and MO decreased with an increase of reaction time, directly demonstrating the dye removal. The excellent sonocatalytic activity of cluster sphere Fe₃O₄/g-C₃N₄ catalyst can be ascribed to the high porosity morphology, and their hybrid structure. It is said that ultrasonic processes can improve the fabrication of the cavitation that include the formation, growth and collapse of microbubbles [23]. Here, the sono-catalytic process is the combined usage of a Fenton-like reaction and ultrasonic irradiation as an advanced oxidation process for dye degradation. The final result of this process is the generation of hot spots that leads to the high pressure and temperature on the catalyst surface. These hot spots form the relevant factor to activate and dissociate H₂O₂ and H₂O molecules. As the result, the strong oxidizing agents and the reactive radical species as OH[•], HO[•]₂ are generated continuously [24].

The synergy effect between the ultrasonic irradiation and the catalyst could explain the accelerating impact of the heterogeneous catalyst. An appropriate electric field at the interface was fabricated through the hybrid structure, and then enhanced the sonocatalytic activity. A possible mechanism for dye degradation could be proposed in chain of reactions as following [17-19]:



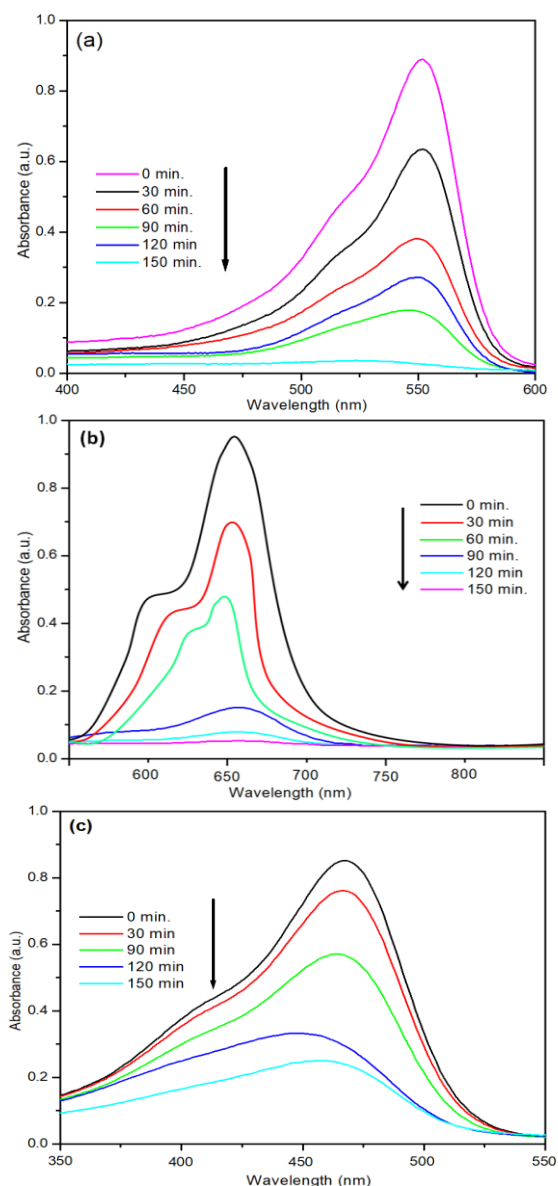


Fig. 4: The UV-Vis absorption of dye during the sonocatalytic degradation: (a) RhB degradation; (b) MB degradation; (c) MO degradation

The stability and reusability of the $\text{Fe}_3\text{O}_4/\text{g-C}_3\text{N}_4$ composites were investigated by the recycle tests in the oxidation process under ultrasonic irradiation. The experimental results depicted in Fig. 5. The results show that the catalysts can easily be separated from the reaction system with an internal magnet. The dyes removal effectively changes a negligible rate after the 4th successive cycles, demonstrating the high reusability of the catalysts (Fig. 5). To further prove the stability of heterogeneous catalysts, leaching iron also was checked by the AAS method. The leaching Fe content was 0.0016, 0.001, 0.0014 mg/L in RhB, MB and MO degradation reaction, respectively. The experimental results revealed that metal content leaching in solution is insignificant. The factors such as

high sonocatalytic activity, stability, and easy separation could improve the application capacity of the as-prepared catalysts for water treatment at industry scale.

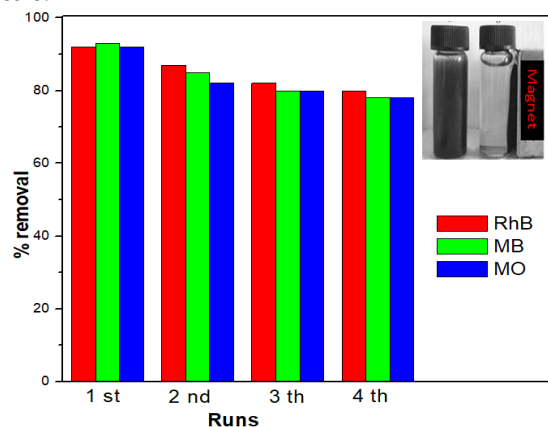


Fig. 5: The stability of the $\text{Fe}_3\text{O}_4/\text{g-C}_3\text{N}_4$ composites after 4 recycles

4. Conclusion

Magnetic separable $\text{Fe}_3\text{O}_4/\text{g-C}_3\text{N}_4$ composite was successfully prepared by simple hydrothermal process. The results showed that $\text{Fe}_3\text{O}_4/\text{g-C}_3\text{N}_4$ composite with added 20% $\text{g-C}_3\text{N}_4$ revealed the high sonocatalytic activity for RhB, MB, and MO degradation in presence of H_2O_2 . The improved sonocatalytic activity of as-prepared $\text{Fe}_3\text{O}_4/\text{g-C}_3\text{N}_4$ can be ascribed to their morphology and hybrid structure. The structure of $\text{g-C}_3\text{N}_4$ and Fe_3O_4 is suitable for adsorption ultrasonic while comparing to a physical mixture of two components. In addition, these composites with a hybrid structure would form a flexible electric field at the interface and then improve the sonocatalytic activity. On the other hand, the integration of H_2O_2 and catalyst dosage are also factors that enhance the sonocatalytic degradation of dyes. Specially, $\text{Fe}_3\text{O}_4/\text{g-C}_3\text{N}_4$ can be collected easily by using an external magnetic field and expose the high stability and high efficiency after four runs. These properties of the Fe_3O_4 cluster sphere/ $\text{g-C}_3\text{N}_4$ composites make them to be a promising catalyst for degrading dye contaminants with H_2O_2 and ultrasonic-assisted.

Ethics declarations

The authors declare that there is no conflict of interest regarding the publication of this paper.

References

1. S. Alamri Rahmah Dhahawi Ahmad, R. Adnan, Wen Da Oh, A. Faiz A. Lati, Alomari Asma Dhahawi Ahmad, International Journal of Biological Macromolecules 229 (2022) 838-848. <https://doi.org/10.1016/j.ijbiomac.2022.12.287>.
2. E. Bartfai, K. Nemeth, B.E. Mrabate, M. Udayakumar, K. Hernadi, Z. Nemeth, J Nanosci Nanotechnol 19 (2019) 422-428. <https://doi.org/10.1166/jnn.2019.15773>
3. Z. Cheng, X. Quan, Y. Xiong, L. Yang, Y. Huang, Ultrason Sonochem, 19 (2012) 1027-1032. <https://doi.org/10.1016/j.ultsonch.2012.02.008>
4. Y.C. Chen, A.V. Vorontsov, P.G. Smirniotis, Photochem Photobiol Sci 2 (2003) 694-698. <https://doi.org/10.1039/b300444a>
5. M. Eghbali-Arani, A. Sobhani-Nasab, M. Rahimi-Nasrabadi, F. Ahmadi, S. Pourmasoud, Ultrason. Sonochem 43 (2018) 120-135. <https://doi.org/10.1016/j.ultsonch.2017.11.040>.
6. P. Gholami, L. Dinpazhoh, A. Khataee, A. Hassani, A. Bhatnagar, J Hazard Mater 381 (2020) 120742. <https://doi.org/10.1016/j.jhazmat.2019.120742>.
7. V. Ramasamy Raja, D. Rani Rosaline, A. Suganthi, M. Rajarajan, Ultrason Sonochem 44 (2018) 73-85. <https://doi.org/10.1016/j.ultsonch.2018.02.010>.
8. S.Y. Hao, Y.H. Li, J. Zhu, G.H. Cui, Ultrason Sonochem 40 (2018) 68-77. <https://doi.org/10.1016/j.ultsonch.2017.06.028>.
9. H. Eskandarloo, A. Badii, M.A. Behnajady, A. Tavakoli, G.M. Ziarani, Ultrason Sonochem 29 (2016) 258-269. <https://doi.org/10.1016/j.ultsonch.2015.10.004>.
10. H. Gao, W. Liu, B. Lu, F. Liu, J Nanosci Nanotechnol 12 (2012) 3959-3965. <https://doi.org/10.1166/jnn.2012.5859>
11. M. Ahmad, E. Ahmed, Z.L. Hong, W. Ahmed, A. Elhissi, N.R. Khalid, Ultrason Sonochem 21 (2014) 761-773. <https://doi.org/10.1016/j.ultsonch.2013.08.014>.
12. D.L. Shun Wang, Zhaojie Wang, Nuo Yu, Haifeng Wang, Zhigang Chen, Lisha Zhang, Materials Letters Vol. 12 (2019) 1950025-1950029. <https://doi.org/10.1142/S1793604719500255>.
13. P. Alimard, Polyhedron 171 (2019) 98-107. <https://doi.org/10.1016/j.poly.2019.06.058>.
14. W. He, Z. Li, S. Lv, M. Niu, W. Zhou, J. Li, R. Lu, H. Gao, C. Pan, S. Zhang, Chemical Engineering Journal 409 (2021) 128274. <https://doi.org/10.1016/j.cej.2020.128274>.
15. N. Zhang, X. Li, Y. Wang, B. Zhu, J. Yang, Ceramics International 46 (2020) 20974-20984. <https://doi.org/10.1016/j.ceramint.2020.05.158>.
16. D. Beketova, M. Motola, H. Sopha, J. Michalicka, V. Cicmancova, F. Dvorak, L. Hromadko, B. Frumarova, M. Stoica, J.M. Macak, ACS Applied Nano Materials 3 (2020) 1553-1563. <https://doi.org/10.1021/acsanm.9b02337>.
17. Shukun Le, Tingshun Jiang, Yiwen Li, Qian Zhao, Yingying Li, Weibing Fang, Ming Gong, Applied Catalysis B: Environmental 200 (2017) 601-610. <https://doi.org/10.1016/j.apcatb.2016.07.027>
18. Lu Ya Chen, Wei De Zhang, Applied Surface Science 301 (2014) 428-435. <https://doi.org/10.1016/j.apsusc.2014.02.093>.
19. X. Wang, W. Mao, J. Zhang, Y. Han, C. Quan, Q. Zhang, T. Yang, J. Yang, X. Li, W. Huang, J Colloid Interface Sci 448 (2015) 17-23. <https://doi.org/10.1016/j.jcis.2015.01.090>.
20. T.S. Ahoovie, N. Azizi, I. Yavari, M.M. Hashemi, Journal of the Iranian Chemical Society 15 (2018) 855-862. <https://doi.org/10.1007/s13738-017-1284-9>.
21. K. Vignesh, A. Suganthi, B.-K. Min, M. Kang, Journal of Molecular Catalysis A: Chemical 395 (2014) 373-383. <https://doi.org/10.1016/j.molcata.2014.08.040>.
22. M. Masjedi-Arani, M. Salavati-Niasari, Ultrason Sonochem 43 (2018) 136-145.
23. R. Mahdavi, S.S. Ashraf Talesh, Materials Chemistry and Physics 267 (2021) 124581. <https://doi.org/10.1016/j.matchemphys.2021.124581>.
24. L. Xu, X.-F. Wang, B. Liu, T. Sun, X. Wang, Colloids and Surfaces A: Physicochemical and Engineering Aspects 627 (2021) 127222. <https://doi.org/10.1016/j.colsurfa.2021.127222>.